Mechanisms of visible photoluminescence in porous silicon

S. Sawada
Department of Electrical and Electronics Engineering, Kagoshima University, 1-21-40 Korimoto, Kagoshima 890, Japan

N. Hamada and N. Ookubo
Fundamental Research Laboratories, NEC Corporation, 34 Miyukigaoka, Tsukuba 305, Japan

(Received 1 October 1993)

We propose a model for porous silicon, an irregular structure obtained by removing some silicon atoms randomly from a perfect silicon crystal. It is shown by using two-dimensional clusters with a tight-binding model that this model exhibits the energy-gap widening and the nonexponential decay of the photoluminescence (PL), which are in good agreement with the observed properties of porous silicon. In this model, the energy-gap widening is due to the localization of eigenstates caused by the randomness of the structure. The distributions in both size and position of the localized eigenstates, i.e., a statistical effect, yield nonexponential PL decay which is describable by the stretched exponential function. A dynamical effect due to electron and hole hopping between the eigenstates explains the observed strong energy dependence of the PL lifetimes.

I. INTRODUCTION

The recent discovery of visible photoluminescence (PL) from porous silicon has stimulated a great deal of interest in this material. There are several proposals for the mechanism of this PL. Canham[1] has suggested the silicon-wire nanocrystal as a porous silicon structure to explain the visible light emission by band-gap widening and relaxation of the momentum selection rule due to the size effect. This idea also has been proposed independently by another group.[2] Cullis and Canham[3] later observed a structure of chained ball-like nanocrystallites rather than pillarlike crystals under an electron microscope. On the other hand, Brandt *et al.*[4] have attributed the origin of the PL to siloxene derivatives present in porous silicon due to the similarity between the PL spectrum of porous silicon and that of siloxene derivatives.

Xie *et al.*[5] have observed a nonexponential PL decay in the microsecond region, and considered this slow decay to be related to some surface states of nanocrystallites. Vial *et al.*[6] have proposed nanocrystallites surrounded by SiO_2 walls as the porous silicon structure. They have explained the observed dependence of PL lifetimes on PL energies in terms of the tunneling of carriers across the SiO_2 wall. The nonexponential PL decay has been well described by the stretched exponential function. Analysis[7] employing this function has shown that the PL decay rate and the nonexponentiality increase with increasing PL energy. In addition to the PL lifetimes in the microsecond region, a diverse range of PL lifetimes ranging from picoseconds to microseconds has been reported.[8,9]

There are several theoretical works, semiempirical[10] and first-principles[11–13] calculations based on the quantum wire model. These works have shown that the quantum wire exhibits both the band-gap widening and the direct gap consistent with the observed PL spectrum. The quantum size effect on excitons in the quantum dot[14] has also been examined, using the effective-mass theory to yield the band-gap widening and the indirect-to-direct conversion of the optical transition.

The calculations for optical matrix elements have provided estimations of radiative lifetimes of localized excitons that indicate they may be larger than a microsecond for the quantum wire,[11] and vary from a nanosecond to a millisecond corresponding to the range of diameters from ~ 1 to ~ 3 nm for the quantum dot.[14] However, the PL decay properties are determined by both radiative and nonradiative processes. The experiment[6] has shown the nonradiative process to be dominant at room temperature. Craig[15] has suggested that the diverse range of PL lifetimes observed in experiments should be related to the localization of electron states in the irregular structure within the porous structure. Gösele and Lehmann,[16] as a result of their absorption experiments, have proposed that porous silicon consists of an interconnected silicon skeleton which implies irregularity of the structure.

In this paper, we propose a primitive structure of porous silicon, an irregular structure obtained by removing some silicon atoms randomly from a perfect silicon crystal. We assume that in this structure most dangling bonds of silicon atoms are terminated by hydrogen atoms, while the remaining dangling bonds act as nonradiative recombination centers for electrons and holes. We consider that Si-H bond formation prevents reconstruction around vacancies.[17] Therefore, this structure partially retains an original crystal symmetry, which is consistent with experimental facts.[18,19] In this structure, a large number of electron states are localized due to randomness of this structure. This results in a reduction of the widths of both valence and conduction bands and, therefore, energy-gap widening. This is demonstrated with two-dimensional Si clusters by using a tight-binding model. In this way, we will show that creating this structure is quite an efficient use of band-gap widening compared to the simple reduction of the crystal size.

In the present model, localized states can exist even in infinite clusters due to the randomness of the structure. This is related to the quantum percolation problem.[20,21] However, we do not devote ourselves to the quantum percolation problem in depth in the present paper.

Based on the above model, and solving master equations describing PL processes, we show that the PL intensity exhibits nonexponential decay closely describable by the stretched exponential function, as experiments[7] have revealed. We consider not only radiative and nonradiative electron-hole recombination, but also electron and hole hopping between their eigenstates via phonon-induced tunneling. The nonradiative recombination is assumed to be a dominant process in the decay of the PL intensity according to experimental facts.[6] We show that the distribution of the nonradiative transition probability, i.e., a statistical effect, causes the stretched exponential decay of the PL intensity, although the PL lifetime and nonexponentiality are not strongly dependent on the PL energy. When the dynamic effect due to electron and hole hopping is taken into account, it especially affects the PL decay, which explains the experimentally observed dependence of PL lifetime on PL energy.[5-7]

In Sec. II, we present the finite two-dimensional cluster model, whose energy gap and eigenstates are calculated by a tight-binding model. The relation between the energy-gap widening and localization of the eigenstates is also shown. In Sec. III, the master equation based on this model is presented with its numerical results. We also discuss the origin of the stretched exponential decay of the PL intensity. The discussion and conclusion are given in Secs. IV and V, respectively.

II. ELECTRONIC STRUCTURE OF POROUS SILICON

We show the energy-gap widening and localization of eigenstates of the porous structures using two-dimensional Si clusters. Electronic states are calculated using the tight-binding model proposed by Pandey and Phillips,[22] which reproduces very well not only the valence band but also the band gap and the bottom of the conduction band of Si in the diamond structure. For interactions between Si and H atoms, Pandey's parameters[23] are used, which reproduce very well the energy levels of SiH_4 and Si_2H_6 molecules.

As can be seen from two-dimensional Si clusters illustrated in the top view of Fig. 1, the structures are generated by fractional and random removals of some atoms. The structure generally contains several mutually independent clusters, among which we choose the largest

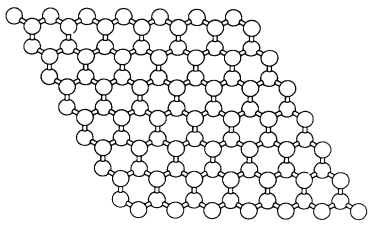

FIG. 1. Two-dimensional Si cluster in top view.

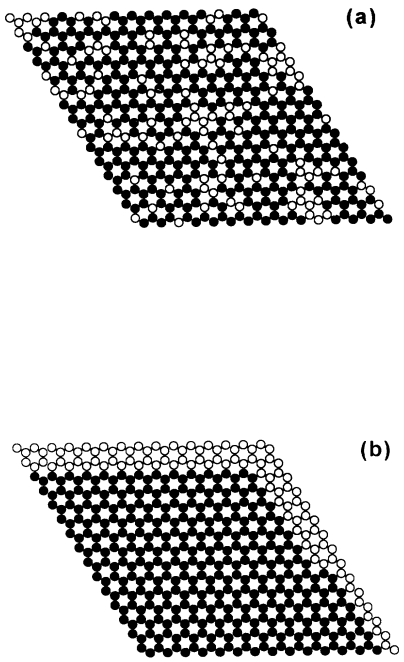

FIG. 2. (a) A Si skeleton of a cluster representing porous silicon consisting of 350 atoms: ●, Si atoms; ○, vacancies. (b) A Si skeleton of a regular cluster consisting of 350 Si atoms: ●, Si atoms; ○, vacancies.

cluster and calculate its electronic states to see the band-gap widening. Smaller clusters generally have larger energy gaps. All dangling bonds of Si atoms are terminated by hydrogen atoms to prevent dangling-bond states from appearing in an energy gap. For simplicity, we neglect the relaxation of silicon atoms from their bulk positions.

For example, the cluster consisting of 350 Si atoms is illustrated in Fig. 2(a), where the black and white circles represent Si atoms and vacancies, respectively. This cluster is the largest one picked up from a structure obtained by a random removal of a fraction 0.2 of Si atoms in an original cluster consisting of 450 Si atoms. The calculated value of the energy gap of this cluster is 2.06 eV. On the other hand, the value of the regular cluster consisting of 350 Si atoms illustrated in Fig. 2(b) is 1.51 eV. A regular cluster means a cluster having smooth facets and no vacancies inside. For comparison, the original cluster, consisting of 450 Si atoms, and the infinite two-dimensional cluster have energy gaps of 1.39 and 1.49 eV, respectively. The results of energy gaps for other exam-

TABLE I. Energy gaps of clusters representing porous silicon and regular clusters.

Fraction	Number of Si atoms	Energy gap (eV) Cluster for porous silicon	Regular cluster
0.3	144	2.393	1.651
0.25	306	2.194	1.525
0.2	350	2.062	1.511
0.15	376	1.858	1.504
0.1	416	1.684	1.493

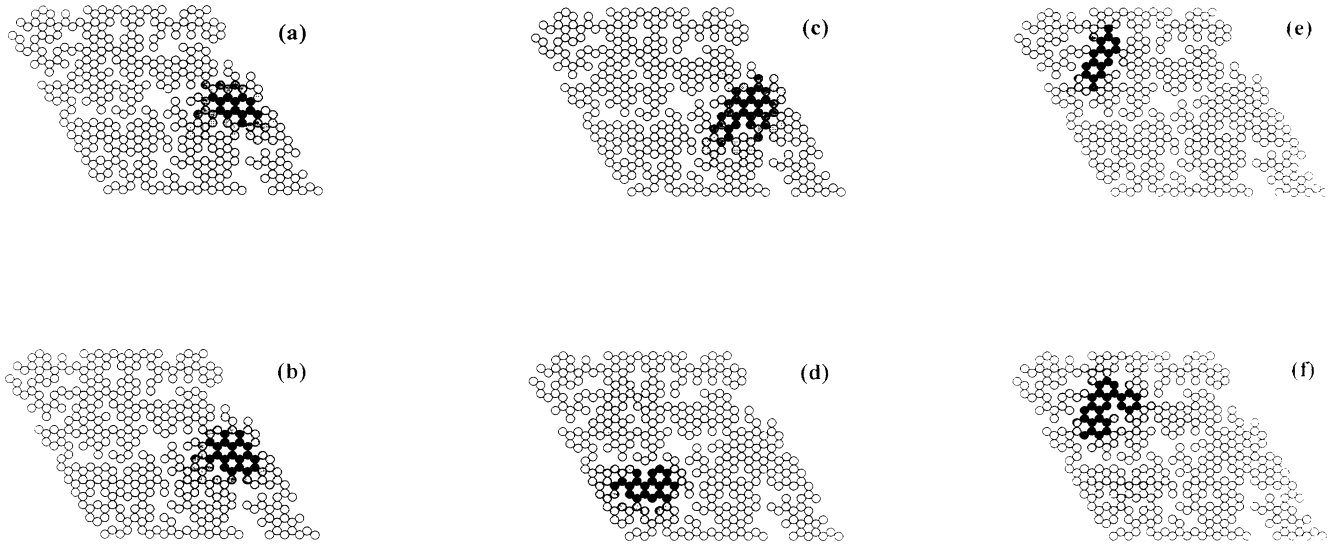

FIG. 3. Amplitudes of the several eigenstates of the porous-silicon cluster consisting of 350 Si atoms; (a) HOMO, (b) LUMO, (c) second HOMO, (d) second LUMO, (e) third HOMO, and (f) third LUMO. The amplitudes are larger at the atoms shaded more darkly. The four classes of shading correspond to the regions of the amplitude from $\frac{1}{2}^{n+1}$ to $\frac{1}{2}^{n}$ of the maximum with $n=0$, 1, 2, and 3.

ples are shown in Table I, in which clusters have been obtained by random removals of Si atoms in various fractions from the original cluster consisting of 450 Si atoms. It can be seen in this table that the clusters generally have larger energy gaps than regular clusters consisting of the same number of Si atoms.

We show that the energy-gap widening of the structure as seen above is related to the localization of the eigenstates. We calculate the amplitude of the nth eigenstate on the ith Si atom defined by

$$P_i^{(n)}=\sum_{\alpha=s,x,y,z}|C_{i,\alpha}^{(n)}|^2+\sum_{j\in i}|C_{Hj}^{(n)}|^2\ , \tag{1}$$

where $C_{i,\alpha}^{(n)}$ is the component of the α-type orbital of the nth eigenstate on the ith Si atom, and $C_{Hj}^{(n)}$ is that on the jth hydrogen atomic orbital. In the second term on the right-hand side of Eq. (1), the summation runs over hydrogen atoms bonded to the ith atom, i.e., the amplitude on each hydrogen atom is assigned to a Si atom bonded to it. The amplitudes of several states [HOMO (highest occupied molecular orbital), LUMO (lowest unoccupied molecular orbital), etc.] for the cluster consisting of 350 Si atoms are illustrated in Fig. 3. Those for the regular cluster are shown in Fig. 4. In these figures, the amplitudes are larger at the atoms shaded more darkly. Comparing Figs. 3 and 4, we see that eigenstates of the cluster representing porous silicon are more localized than those of the regular cluster.

In order to examine in detail the degree of the localization of the eigenstates, we calculate the participation ra-

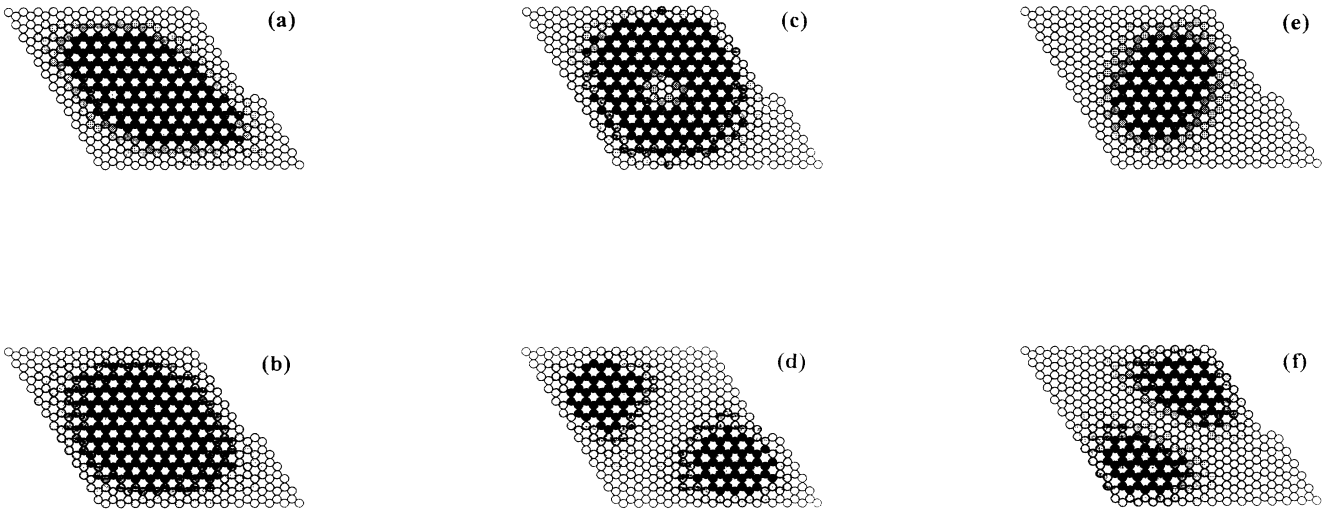

FIG. 4. The same as Fig. 3, except for the regular cluster consisting of 350 Si atoms.

tio[24] of the nth eigenstate define by

$$y^{(n)}=\left[N\sum_i (P_i^{(n)})^2\right]^{-1}, \quad (2)$$

where N is the number of Si atoms. If a state is localized on M Si atoms, $y^{(n)}\sim M/N$, since $P_i^{(n)}\sim M^{-1}$. The results for $y^{(n)}$ around Fermi levels are shown in Figs. 5(a) and 5(b) for the porous cluster, and in Figs. 6(a) and 6(b) for the regular cluster. Comparing Figs. 5 and 6, we see that the cluster representing porous silicon, having a wider energy gap, exhibits much more localization of the eigenstates than the regular cluster. Moreover, it can be seen in Fig. 5 that in this cluster the degree of localization varies irregularly from state to state. The position of the localization center also varies from state to state. In particular, relatively extended states appear irregularly over a whole range of energy. The amplitudes for two examples of the extended states, which are indicated in Figs. 5(a) and 5(b) by arrows, are illustrated in Figs. 7(a) and 7(b), respectively. This feature is in contrast to the case of the regular cluster: Most of states are delocalized in almost the same degree. The distributions in both positions and sizes of the localized eigenstates yield a large variety of nonradiative transition probabilities. This causes the nonexponential decay of the PL intensity as shown below.

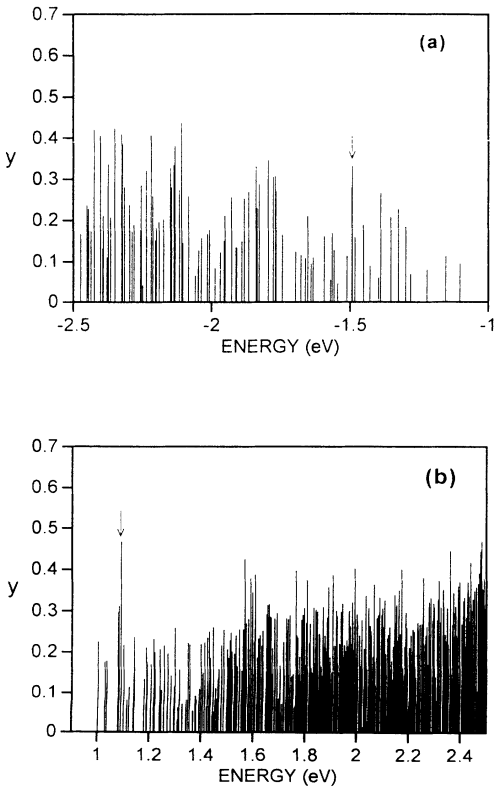

FIG. 5. (a) and (b) Participation ratios of the eigenstates around the Fermi level for the porous-silicon cluster. The arrows indicate extended states whose amplitudes are illustrated in Fig. 17.

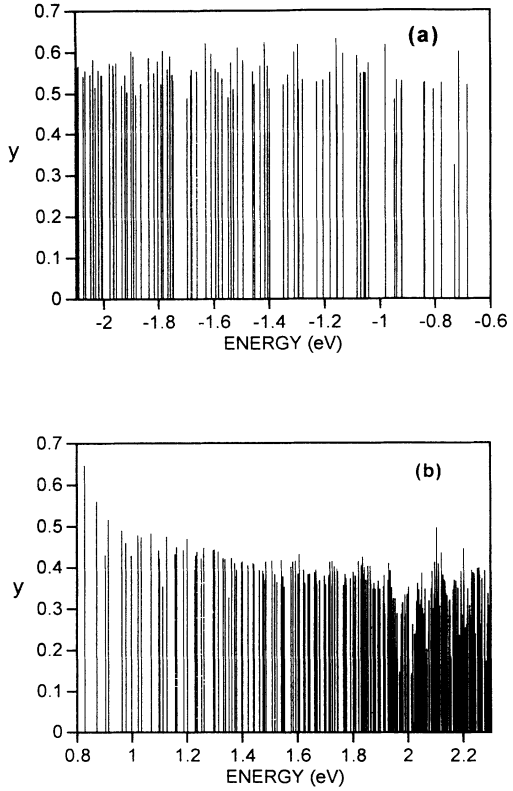

FIG. 6. (a) and (b) The same as Fig. 5, except for the regular cluster.

III. TIME EVOLUTION OF PL INTENSITY

A. Master equations

Now we proceed to discussions of the time evolution of PL intensity on the above model. After electrons are excited from lower occupied levels to upper unoccupied lev-

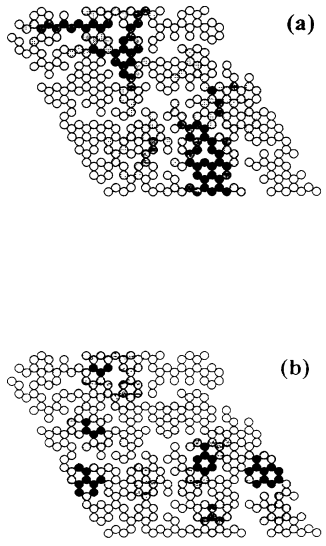

FIG. 7. The amplitudes of (a) the thirteenth HOMO and (b) the eighth LUMO for the porous-silicon cluster, which are indicated by the arrows in Fig. 5.

els, both electrons and holes hop between localized or extended eigenstates via phonon-induced tunneling. This process is described by the master equations[25] for the occupation numbers of the eigenstates:

$$\frac{dn_i}{dt}=\sum_j \gamma_{ij}(1-n_i)n_j-\sum_j \gamma_{ji}(1-n_j)n_i \ , \tag{3}$$

where n_i is an occupation number of the ith eigenstates, and γ_{ij} a transition probability from the jth eigenstate to the ith one. Assuming weak coupling between electron and phonon, we use the following model[26–28] for the transition probabilities:

$$\gamma_{ij}=\begin{cases}\gamma_0 S_{ij}e^{-\eta|E_i-E_j|/\hbar\omega_{\rm ph}}e^{-(E_j-E_i)/kT}, & \text{for } E_j>E_i\\ \gamma_0 S_{ij}e^{-\eta|E_i-E_j|/\hbar\omega_{\rm ph}}, & \text{for } E_j<E_i \ ,\end{cases} \tag{4}$$

where E_i is the energy of the ith eigenstate, T is the temperature, and k is the Boltzmann constant. The S_{ij} is an overlap defined by

$$S_{ij}=\sum_l P_l^{(i)}P_l^{(j)} \ , \tag{5}$$

where the summation runs over all Si atoms and $P_l^{(i)}$ is defined by Eq. (1). The multiphonon process is reflected by the factor $\exp(-\eta|E_i-E_j|/\hbar\omega_{\rm ph})$, i.e., the exponential dependence on the phonon number, $|E_i-E_j|/\hbar\omega_{\rm ph}$, where $\omega_{\rm ph}$ is a maximum phonon frequency. The coefficient η depends weakly on the temperature, and is of order of unity. We use $\eta=1$ for simplicity. The γ_0 is an electron-phonon-coupling constant independent of the energy. This model of γ_{ij} satisfies the detailed balance condition:

$$\begin{aligned}&\gamma_{ij}(1-\bar{n}_i)\bar{n}_j=\gamma_{ji}(1-\bar{n}_j)\bar{n}_i \ ,\\ &\bar{n}_i=[1+\exp(E_i/kT)]^{-1} \ .\end{aligned} \tag{6}$$

In addition to the above process, there are two kinds of processes for electron-hole recombination: radiative recombination and nonradiative recombination. The former results in photoluminescence. We consider the latter to proceed as follows: electrons (holes) lose their energies through electron-phonon interaction, and are trapped in dangling bonds, and then holes (electrons) move nearby to recombine. This process also can be described by Eq. (3) with different transition probabilities γ'_{ij} given[26–28] by

$$\gamma'_{ij}=\begin{cases}\gamma'_0 S_{ij}e^{-\Delta E_{ij}/kT}e^{-(E_j-E_i)/kT}, & \text{for } E_j>E_i\\ \gamma'_0 S_{ij}e^{-\Delta E_{ji}/kT}, & \text{for } E_j<E_i \ ,\end{cases} \tag{7}$$

where ΔE_{ij} is the activation energy for the transition from the jth to the ith states, and γ'_0 is an electron-phonon-coupling constant independent of the energy. This expression can be derived from the assumption of strong coupling between electron and phonon. The dangling-bond states are introduced by removing some hydrogen atoms terminating dangling bonds. The radiative recombination is described by adding new terms to the right-hand side of Eq. (3). We rewrite the electron occupation numbers as $n_i^{(e)}(=n_i)$ for electrons in upper levels as $n_i^{(h)}(=1-n_i)$ for holes in lower levels, and as $n_i^{(d)}(=n_i)$ for electrons in the dangling-bond state. The equations for these numbers are given by

$$\begin{aligned}\frac{dn_i^{(e)}}{dt}=&\sum_j \gamma_{ij}(1-n_i^{(e)})n_j^{(e)}-\sum_j \gamma_{ji}(1-n_j^{(e)})n_i^{(e)}\\ &+\sum_j \gamma'_{ij}(1-n_i^{(e)})n_j^{(d)}\\ &-\sum_j \gamma'_{ji}(1-n_j^{(d)})n_i^{(e)}-\sum_j \alpha_{ij}n_i^{(e)}n_j^{(h)} \ ,\end{aligned} \tag{8}$$

$$\begin{aligned}\frac{dn_i^{(h)}}{dt}=&\sum_j \gamma_{ji}(1-n_i^{(h)})n_j^{(h)}-\sum_j \gamma_{ij}(1-n_j^{(h)})n_i^{(h)}\\ &+\sum_j \gamma'_{ji}(1-n_i^{(h)})(1-n_j^{(d)})\\ &-\sum_j \gamma'_{ij}n_j^{(d)}n_i^{(h)}-\sum_j \alpha_{ij}n_i^{(h)}n_j^{(e)} \ ,\end{aligned} \tag{9}$$

and

$$\begin{aligned}\frac{dn_i^{(d)}}{dt}=&\sum_j \gamma'_{ij}(1-n_i^{(d)})n_j^{(e)}-\sum_j \gamma'_{ji}(1-n_j^{(e)})n_i^{(d)}\\ &+\sum_j \gamma'_{ij}(1-n_i^{(d)})(1-n_j^{(h)})\\ &-\sum_j \gamma'_{ji}n_j^{(h)}n_i^{(d)} \ ,\end{aligned} \tag{10}$$

respectively. The last terms in the right-hand sides of Eqs. (8) and (9) represent the electron-photon interaction. α_{ij} is assumed to have the following form:

$$\alpha_{ij}=\alpha_0 S_{ij} \ , \tag{11}$$

where α_0 is the electron-photon-coupling constant independent of energies, and S_{ij} is the overlap defined by (5). Equations (8)–(10) are solved with the initial conditions

$$n_i^{(e)}(t=0)=A\sum_j \alpha_{ij}\exp\{-\sigma[E_0-(E_i-E_j)]^2\} \ , \tag{12}$$

$$n_i^{(h)}(t=0)=A\sum_j \alpha_{ji}\exp\{-\sigma[E_0-(E_j-E_i)]^2\} \ , \tag{13}$$

and

$$n_i^{(d)}(t=0)=0.5 \ , \tag{14}$$

where E_0 and σ are parameters. The constant A is determined by a total number of excited electrons. The PL intensity is given by

$$I(E,t)=\sum_i\sum_j \alpha_{ij}n_i^{(e)}n_j^{(h)}\delta[E-(E_i-E_j)] \ . \tag{15}$$

Equations (8–10) are solved numerically with a cluster consisting of 151 Si atoms, as illustrated in Fig. 8, in which a hydrogen atom bonded to each shadowed Si atom is removed to introduce two dangling bonds. The eigenenergies E_i and the overlaps S_{ij} for this cluster are calculated by the tight-binding model. We chose the De-

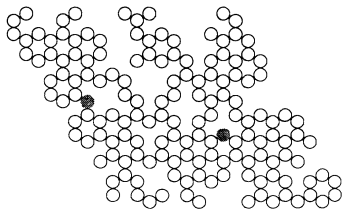

FIG. 8. A Si skeleton of a porous-silicon cluster consisting of 151 Si atoms. A hydrogen atom bonded to each shadowed atom is removed.

bye frequency for silicon in the diamond structure to be the phonon frequency $\omega_{\rm ph}$. Hereafter, we treat only the case of the temperature $T=300$ K. We assume the activation energies ΔE_{ij} to be constant for simplicity. Then the exponential factor $\exp(-\Delta E_{ij}/kT)$ can be included in the coupling constant γ_0', since we are not concerned in this paper with the temperature dependence of the PL intensity.

B. Stretched exponential decay

Before presenting numerical results for Eqs. (8)–(10), we show that the distribution of the nonradiative transition probability (statistics) causes the stretched exponential decay of the PL intensity. This stretched exponential behavior is preserved even under the dynamical effect due to the electron and hole hopping, although it is somewhat modified, as shown in Sec. III C.

We assume according to experimental fact[6] that nonradiative recombination is a dominant process in the relaxation of the PL intensity, and that the radiative recombination acts only as a perturbation. Now we ignore the electron and hole hopping process and set $\gamma_0=\alpha_0=0$ and $n_i^{(d)}=0.5$ in Eqs. (8) and (9). [Equation (10) is ignored.] We consider initial conditions such that all electron and hole states have the same occupation number initially, i.e., $\sigma=0$. Then we obtain the time evolution of the occupation numbers of electrons and holes to be $n_i^{(e)}\propto\exp(-\lambda_i t)$ and $n_i^{(h)}\propto\exp(-\lambda_i t)$, respectively, where the decay constant λ_i is given by the sum of the nonradiative transition probabilities γ_{ij}'. The time evolution of the PL intensity can be written as

$$I(E,t)\propto\sum_i\sum_j\alpha_{ij}\exp[-(\lambda_i+\lambda_j)t]\delta[E-(E_i-E_j)]$$
$$\propto\int_0^\infty g(\lambda)\exp(-\lambda t)d\lambda\ , \tag{16}$$

where $g(\lambda)$ is the distribution function of the decay constant λ given by

$$g(\lambda)=\sum_i\sum_j\alpha_{ij}\delta[E-(E_i-E_j)]\delta[\lambda-(\lambda_i+\lambda_j)]\ . \tag{17}$$

In the numerical calculations, the function $\delta[E-(E_i-E_j)]$ in Eqs. (16) and (17) is replaced by the Gaussian function $(\pi/\sigma)^{-1/2}\exp(-\sigma[E-(E_i-E_j)]^2)$, with $\sigma=10\ \text{eV}^{-2}$. Hereafter, we use $\gamma_0'=1$, i.e., times are scaled by $\gamma_0'^{-1}$. Figures 9–11(a) show the time evolution of the PL intensity given by Eq. (16) for the PL energies $E=2.5$, 3.0, and 3.5 eV (the solid curves), respectively,

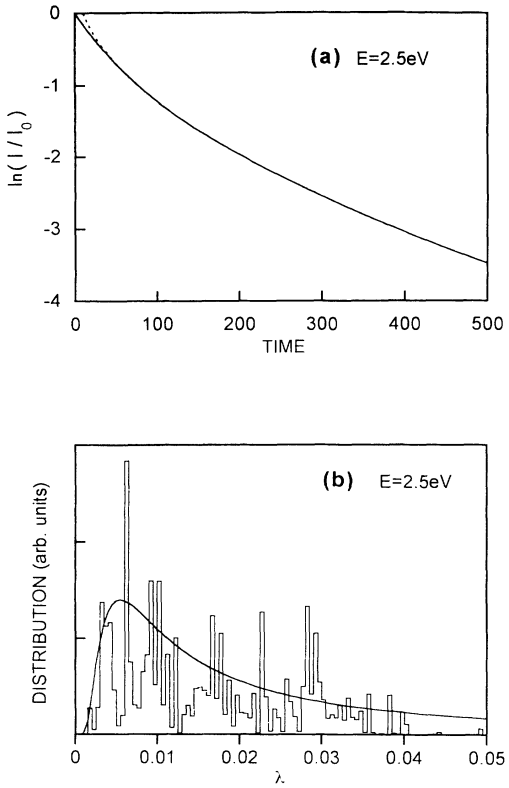

FIG. 9. (a) Time evolution of the PL intensity for the PL energy $E=2.5$ eV: the one given by Eq. (16) (solid curves), and the fitting with the stretch exponential function (broken curves). (b) Distributions of the decay constant λ for the PL energy $E=2.5$ eV: the histogram calculated by Eq. (19) and the fitting with function (18) (a solid curve).

and the fittings with the stretched exponential function $\exp[-(t/\tau)^\beta]$ (the broken curves). We see in these figures that the fittings are very good in the time region $t>50$. The fitting for $E=4.0$ and 4.5 eV are also very good for $t>50$. The values of β and τ are plotted by the crosses in Fig. 12. It can be seen that without the electron and hole hopping process, both β and τ are not dependent on the PL energy. On the other hand, the dynamical effect due to electron and hole hopping yields the strong energy dependence of both β and τ, as seen in Sec. III C.

The histograms in Figs. 9–11(b) represent the distribution of the decay constant λ calculated by Eq. (17). Equation (16) shows that the time evolution of the PL intensity is given by the Laplace transform of the distribution function $g(\lambda)$. Therefore, $g(\lambda)$ for the stretched exponential decay is given by the inverse Laplace transformation of $\exp[-(t/\tau)^\beta]$. Its asymptotic form is obtained by using the saddle-point method:[29]

$$g(\lambda)=\frac{\nu\tau_0}{\sqrt{2\pi\beta}}(\lambda\tau_0)^{-1-\nu/2}\exp[-(\lambda\tau_0)^{-\nu}]\ , \tag{18}$$

where

$$\nu=\beta(1-\beta)^{-1}\ , \tag{19}$$

$$\tau_0=\tau[\beta(1-\beta)^{1/\nu}]^{-1}\ . \tag{20}$$

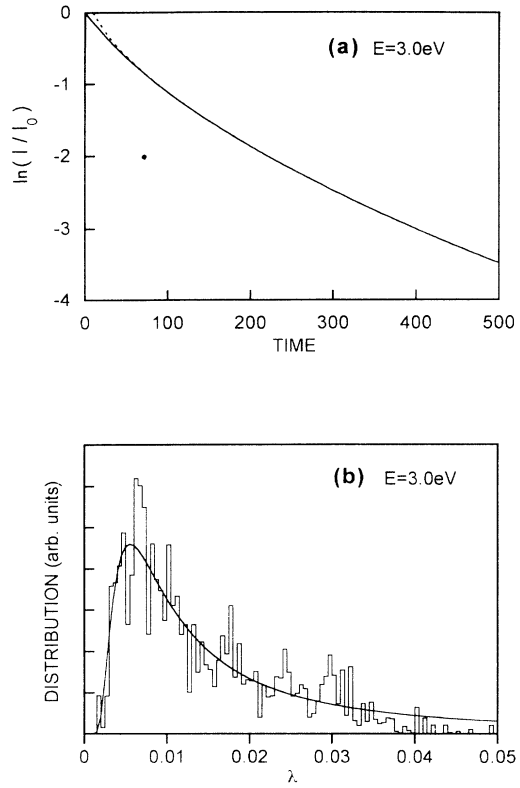

FIG. 10. The same as Fig. 9, except for $E=3.0$ eV.

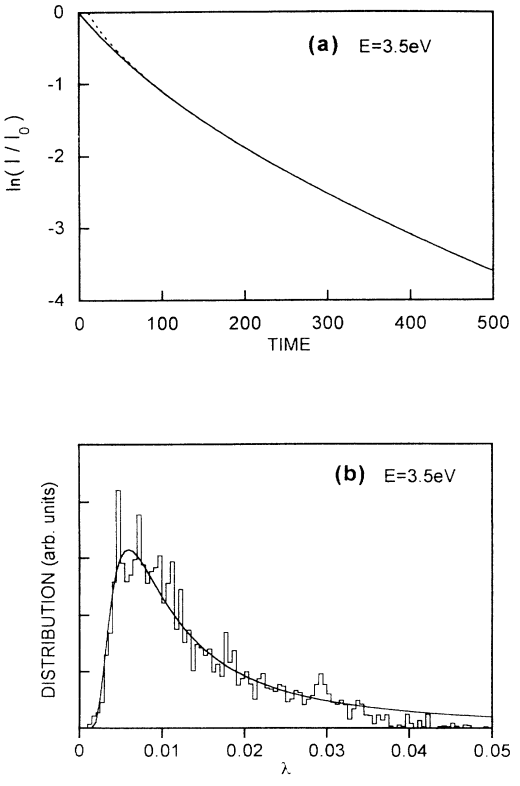

FIG. 11. The same as Fig. 9, except for $E=3.5$ eV.

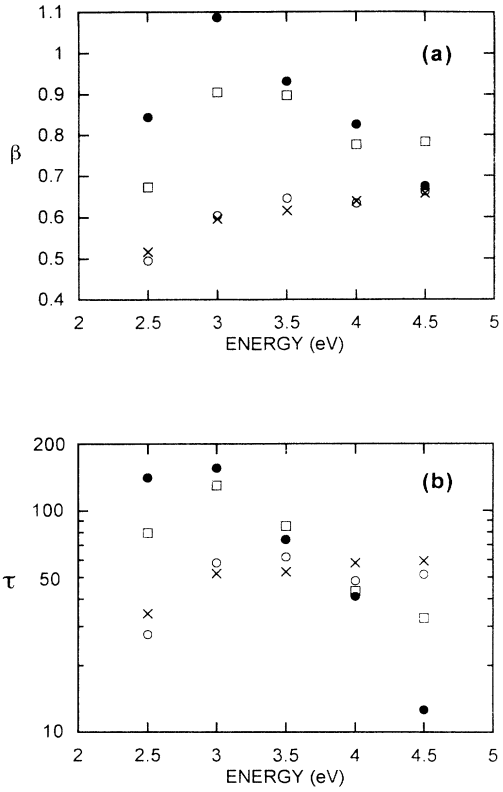

FIG. 12. The parameters β and τ of the stretched exponential decay as functions of the PL energy: ○, $\gamma_0=0$; □, $\gamma_0=0.5$; ●, $\gamma_0=1$; ×, the simplified calculations with $\gamma_0=0$.

Function (18), with the same values of β and τ as used in the fitting of $I(E,t)$, is plotted by the broken curves in Figs. 9–11(b). It can be seen that the histograms for $E=3.0$ and 3.5 eV fit very well with function (18) for $\lambda<0.035$. On the other hand, the fittings are not very good for $\lambda>0.035$, which corresponds to the deviations of $I(E,t)$ from the stretched exponential function in the short-time region $t<50$. This is also the case for $E=4.0$ and 4.5 eV. For $E=2.5$ eV, the fitting of the histogram with function (18) is very poor, and the values of β and τ deviate from those for other energies, though the fitting of $I(E,t)$ with the stretched exponential function is rather good. We consider this to be due to statistical error, i.e., in the present small cluster the number of electron and hole states contributing to this PL energy component is insufficient for this to be regarded as statistically correct.

C. Dynamical effect

Now we take into account the dynamical effect due to electron and hole hopping by solving Eqs. (8)–(10) numerically. Times are scaled by $\gamma_0'^{-1}$. We use $\alpha_0=10^{-3}$. We have found that the results are insensitive to the value of α_0 as long as α_0 is sufficiently smaller than γ_0', e.g., $\alpha_0=10^{-2}$. We vary the value of γ_0 to examine the effect of electron and hole hopping. Finally, we choose $E_0=3.0$ eV and $\sigma=10$ eV^{-2} in Eqs. (12) and (13), assum-

ing a total number of exited electrons to be equal to 12. We have found that the decay property of the PL intensity is insensitive to a total number of exited electrons. This is due to the following: $n_i^{(e)} \ll 1$ and $n_i^{(h)} \ll 1$ for almost all of the eigenstates, and $n_i^{(d)}$ is nearly equal to 0.5 at any time. Therefore, Eqs. (8) and (9) are almost linear except for the last terms representing the radiative recombination, which act only as a perturbation.

The results of the time evolution of the PL intensities for $\gamma_0=0$, 0.5, and 1 are shown in Figs. 13, 14, and 15, respectively. The δ function in Eq. (15) has been replaced by the Gaussian function $(\pi/\sigma)^{-1/2}\exp(-\sigma E^2)$, with $\sigma=10\ \mathrm{eV}^{-2}$. The PL intensities are given in Figs. 13(a), 14(a), and 15(a) as functions of the PL energy, where the different curves correspond to different times. On the other hand, they are given in Figs. 13(b), 14(b), and 15(b) as functions of time, where the different curves correspond to different PL energies. In the latter plots, the curves can be fitted in the region $t \geq 50 \sim 100$ with the stretched exponential function $\exp[-(t/\tau)^{\beta}]$, using different values of β and τ for different PL energies. In the short-time region $t < 50 \sim 100$, the curves deviate slightly from the stretched exponential function, similarly to Figs. 9–11(a).

The values of β and τ are plotted in Figs. 12(a) and 12(b), respectively, where white circles, squares, and

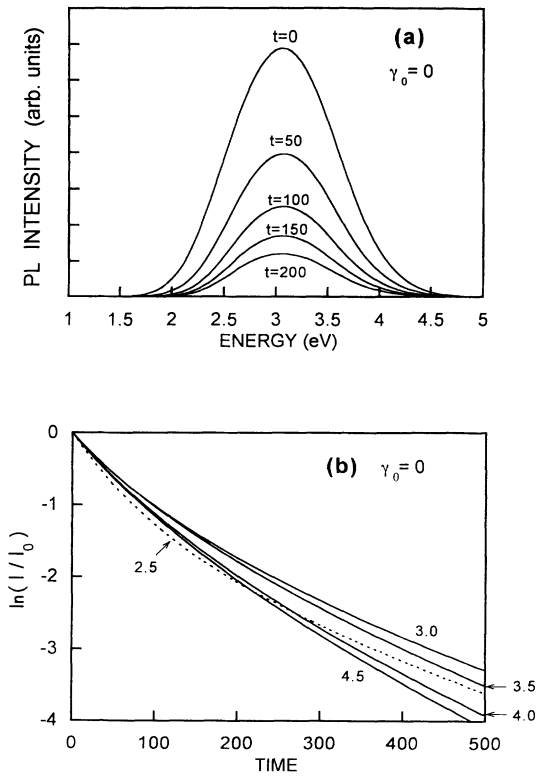

FIG. 13. Time evolution of the PL intensities for $\gamma_0=0$ obtained by solving Eqs. (8)–(10): (a) PL intensities at various times as functions of the PL energy (the values beside the curves indicate times); (b) those for the various PL energies as functions of time (the values beside the curves indicate PL energies in eV). Time is scaled by $\gamma_0'^{-1}$.

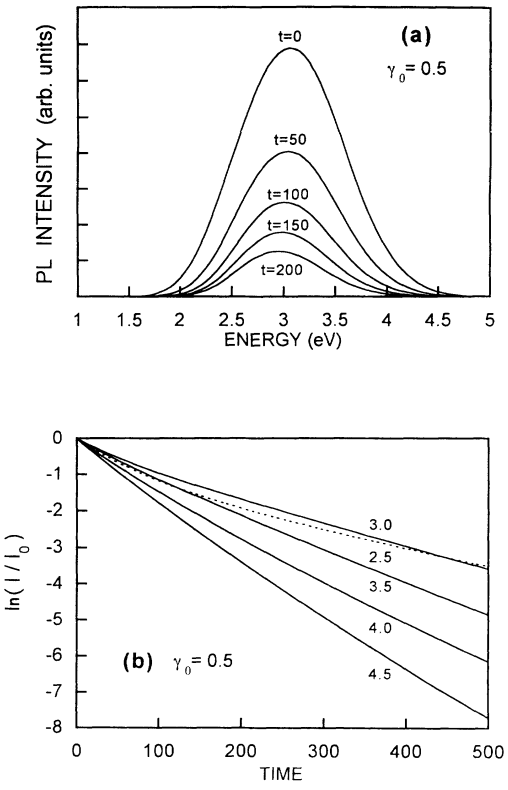

FIG. 14. The same as Fig. 13, except for $\gamma_0=0.5$.

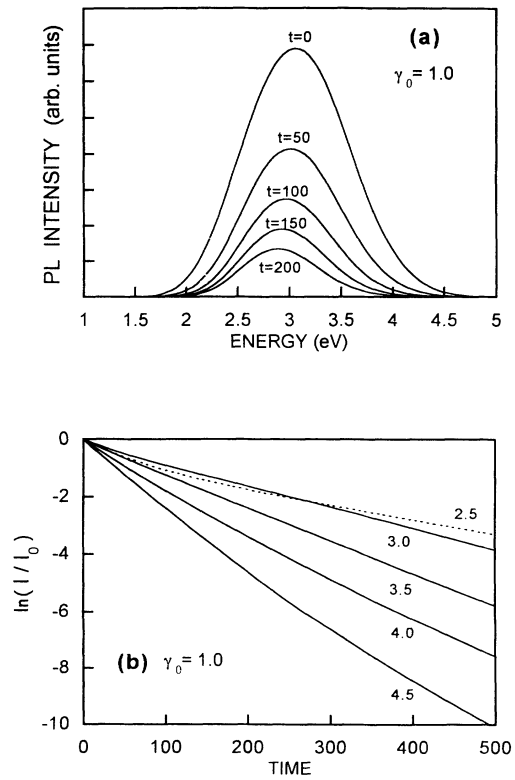

FIG. 15. The same as Fig. 13, except for $\gamma_0=1$.

black circles represent results for $\gamma_0=0$, 0.5, and 1, respectively. The most remarkable feature is that both β and τ depend strongly on the PL energy in the case of $\gamma_0\neq 0$, in contrast to that of $\gamma_0=0$. In particular, τ has an exponential dependence on the energy in the region of $E\geq 3$ eV. These tendencies for $\gamma_0\neq 0$ are in good agreement with the experimental behavior of the PL intensity.[5-7] The deviation from the above tendency at $E=2.5$ eV is due to statistical error, as already mentioned.

In order to understand the origin of the energy dependence of β and τ, we examine in detail the time evolution of the occupation numbers for electrons and holes. The time evolution of the logarithm of the occupation numbers for electrons $n_i^{(e)}$ in the energy region, $0<E<3.0$ eV, is shown for several eigenstates in Figs. 16(a) and 16(b) for $\gamma_0=0$ and 1, respectively, where lower-energy states have larger occupation numbers at $t=0$. Those for holes have similar behavior, and have not been shown. In these figures, the slope of each curve is equal to the decay rate of each state. In Fig. 16(a), slopes of the curves vary over a somewhat wide range, which means that the occupation number of each eigenstate decays with its own rate determined only by the nonradiative transition. This results in the stretched exponential decay of the PL intensity, with β much less than unity. On the other hand, the slope of the curves in Fig. 16(b) varies over a narrower range. This is due to the following fact: Electron and hole hopping forces the system into the local thermal equilibrium, i.e., the rapid decreases in occupation numbers of states having large nonradiative decay rates are suppressed by electrons or holes flow from neighboring states having smaller nonradiative decay rates, and vice versa. As a result, the decay rates of the states become close to each other, so that the PL intensity decays with β closer to unity. The values of β are larger for lower PL energy components, since they are contributed from the smaller range of the eigenstates and, therefore, have a smaller variety of the decay rate. In particular, as seen in Fig. 16(b), there are low-energy states whose occupation numbers themselves decay as $\exp[-(t/\tau)^{\beta}]$ with $\beta>1$. This is due to the large electron flow from higher states, which initially exceeds the proper decay rates of the low-energy states. This also causes the decay of the PL intensity with $\beta>1$.

Electron and hole hopping causes the values of τ to be smaller for the higher PL energy components. This is because the cascade of electrons (holes) from higher (lower) to lower (higher) states makes the lifetime of the higher (lower) states shorter. As a result, the higher PL energy components come to decay faster. The above situation also occurs in the PL energy component of 2.5 eV, i.e., the values of β and τ for $\gamma_0\neq 0$ are larger than those for $\gamma_0=0$. However, even in the case of $\gamma_0\neq 0$, the values of β and τ for $E=2.5$ eV are smaller than those for $E=3.0$ eV.

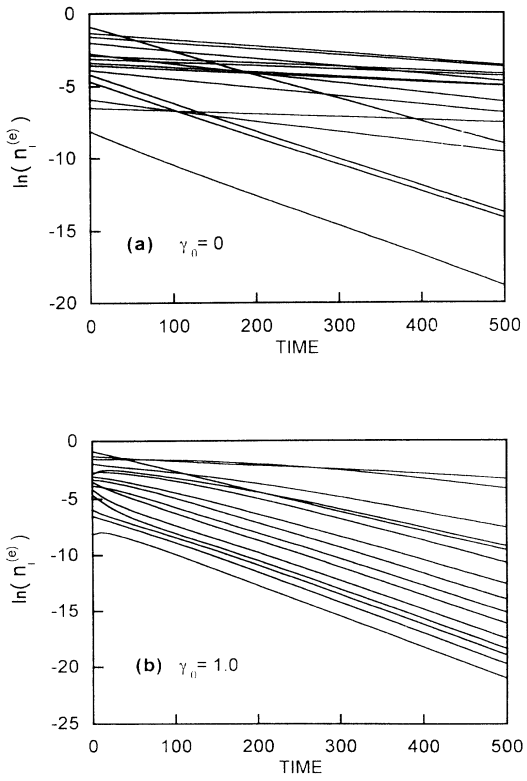

FIG. 16. Time evolution of logarithms of the electron occupation numbers for several eigenstates $n_i^{(e)}$ for (a) $\gamma_0=0$ and (b) $\gamma_0=1$.

IV. DISCUSSION

A structure representing porous silicon may be regarded as a set of component subclusters, which are less irregular than the whole. For example, the cluster illustrated in Fig. 2(a) can be divided into several subclusters as illustrated in Fig. 17. It might be expected that eigenstates of the whole cluster are given by a sum of eigenstates of the subclusters. This is partially true, though the way of the division into subclusters is not unique. Indeed, as seen in Fig. 3, both the LUMO and HOMO are localized almost within the largest subcluster A in Fig. 17. The second and third LUMO's, illustrated in Figs. 3(e) and 3(f), respectively, can be regarded as hybridized states between LUMO's of subclusters B and C. However, this point of view is not very helpful in analyzing the whole electronic structure of the porous cluster. Moving from LUMO to higher states, or from HOMO to lower states, we have greater numbers of degenerated states of subclusters, and the situation is too complicated to be explained in terms of the hybridization. [For example, see Figs. 7(a) and

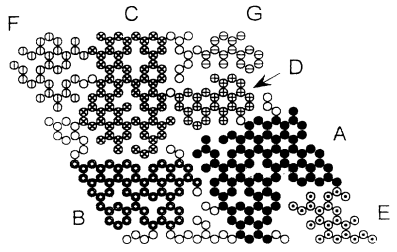

FIG. 17. Subclusters in the porous-silicon cluster consisting of 151 Si atoms. Different subclusters are marked differently.

7(b).] Moreover, even states localized almost within some of the subclusters are somewhat extended to others in reality. This yields a wide distribution for overlaps of eigenstates with dangling-bond states and, therefore, a wide distribution for nonradiative recombination rates.

As seen in Sec. III, the PL decay in a very short-time region is not fitted very well with the stretched exponential function, while experiments[7] have shown very good fittings in a whole time region. We can consider this discrepancy to be due to statistical errors. The present cluster has small numbers of both subclusters and dangling bonds in it, so that the values of the overlaps of the eigenstates with the dangling-bond states and, therefore, the nonradiative transition probabilities are limited somewhat in a narrow region. In particular, it lacks large values for nonradiative transition probabilities. If a cluster is large enough to have a wide variety of subclusters in size, and a large number of dangling bonds at various sites, it could have a diverse range of decay constants to exhibit the stretched exponential PL decay in a whole time region.

Finally, we discuss the time scale of the PL decay. The coupling constant γ_0' is[30-32] of the order of 10^{13} s^{-1}. Therefore, the present model has the decay time $\tau \sim 50\gamma_0'^{-1} \sim 5\times 10^{-12}$ s (see Fig. 12), while experimentally τ is of the order of a microsecond. It should be noted that the decay time is proportional to a density of dangling bonds. In the present model, $N_d/N_{\mathrm{Si}} = \frac{2}{151} \sim 10^{-2}$, where N_{Si} and N_d are the densities of Si atoms and dangling bonds, respectively. In the realistic system, $N_d \sim 10^{-17}$ cm^{-3} if we assume it is of the same order as that in amorphous silicon.[31,32] Since $N_{\mathrm{Si}} \sim 10^{-23}$ cm^{-3}, we have $N_d/N_{\mathrm{Si}} \sim 10^{-6}$ and, therefore, $\tau \sim 0.05$ μs for the realistic system. Now, remembering that γ_0' includes the factor $\exp(-\Delta E_{ij}/kT)$, and assuming $\Delta E_{ij} \sim 0.1$ eV, we have $\exp(-\Delta E_{ij}/kT) \sim 0.01$ for the room temperature and $\tau \sim 5$ μs, which is comparable with experimental results.[5-7] In this way, the present theory can reproduce the realistic time scale for the PL decay.

V. CONCLUSION

We have proposed a model of the porous silicon structure. The model exhibits the energy-gap widening and stretched exponential decay of the PL intensity, which are characteristic features of porous silicon. The energy-gap widening is due to the localization of the eigenstates caused by the randomness of the structure, which brings about an effect similar to the size effect. Various degrees of localization of the eigenstates at various positions yield a wide distribution of nonradiative recombination rates, which is a cause of the stretched exponential decay of the PL intensity. The observed exponential dependence of the lifetime on the PL energy has been explained in terms of the dynamical effect due to electron and hole hopping.

Though the present calculations have been limited to the two-dimensional small clusters, the essential features of the porous silicon structure have been revealed. The present model contains only silicon and hydrogen atoms, while experiments[6] have pointed out the importance of the role of oxygen atoms in porous silicon. This is a problem left for the future. We believe that the present model provides a good guide to better understanding the structure and the properties of porous silicon.

[1] L. T. Canham, Appl. Phys. Lett. **57**, 1046 (1990).
[2] V. Lehmann and U. Gösele, Appl. Phys. Lett. **58**, 856 (1991).
[3] A. G. Cullis and L. T. Canham, Nature (London) **353**, 335 (1991).
[4] M. S. Brandt *et al.*, Solid State Commun. **81**, 307 (1992).
[5] Y. H. Xie *et al.*, J. Appl. Phys. **71**, 2403 (1992).
[6] J. C. Vial *et al.*, Phys. Rev. B **45**, 14 171 (1992).
[7] N. Ookubo *et al.*, Appl. Phys. Lett. **61**, 940 (1992).
[8] S. Gardelis *et al.*, Appl. Phys. Lett. **59**, 2118 (1991).
[9] T. Matsumoto *et al.*, Jpn. J. Appl. Phys. Lett. **31**, L619 (1992).
[10] G. D. Sanders and Y. C. Chang, Phys. Rev. B **45**, 9202 (1992).
[11] A. J. Read *et al.*, Phys. Rev. Lett. **69**, 1232 (1992).
[12] F. Buda, J. Kohanoff, and M. Parrinello, Phys. Rev. Lett. **69**, 272 (1992).
[13] T. Ohno, K. Shiraishi, and T. Ogawa, Phys. Rev. Lett. **69**, 2400 (1992).
[14] T. Takagahara and K. Takeda, Phys. Rev. B **46**, 15 578 (1992).
[15] B. I. Craig, Surf. Sci. **285**, L486 (1993).
[16] V. Gösele and V. Lehmann, in *Extended Abstracts of the 1992 International Conference on Solid State Devices and Materials, Tsukuba, Japan,* edited by Y. Nannichi (The Japan Society of Applied Physics, Tokyo, 1992), p. 469.
[17] T. D. Moustakas, J. Electron. Mater. **8**, 391 (1979).
[18] K. Barla *et al.*, J. Cryst. Growth **68**, 727 (1984).
[19] H. Sugiyama and O. Nittono, J. Cryst. Growth **103**, 156 (1990).
[20] S. Kirkpatrick and T. P. Eggarter, Phys. Rev. B **6**, 3598 (1972).
[21] T. Odagaki, N. Ogita, and H. Matsuda, J. Phys. C **13**, 189 (1980).
[22] K. C. Pandey and J. C. Phillips, Phys. Rev. B **13**, 750 (1976).
[23] K. C. Pandey, Phys. Rev. B **14**, 1557 (1976).
[24] F. Wegner, Z. Phys. B **36**, 209 (1980).
[25] H. Bottger and V. V. Bryksin, *Hopping Conduction in Solids* (VCH, Berlin, 1985), Chap. 1.
[26] R. Englman and J. Jortner, Mol. Phys. **18**, 145 (1970).
[27] N. Robertson and L. Friedman, Philos. Mag. **33**, 753 (1976).
[28] N. F. Mott and E. A. Davis, *Electronic Processes in Non-Crystalline Materials* (Clarendon, Oxford, 1979).
[29] R. Saito and K. Murayama, Solid State Commun. **63**, 625 (1987).
[30] C. W. Struck and W. H. Fonger, J. Lumin. **10**, 1 (1975).
[31] C. Tsang and R. A. Street, Philos. Mag. B **37**, 601 (1978).
[32] I. Hirabayashi, K. Morigaki, and S. Nitta, J. Phys. Soc. Jpn. **50**, 2961 (1981).

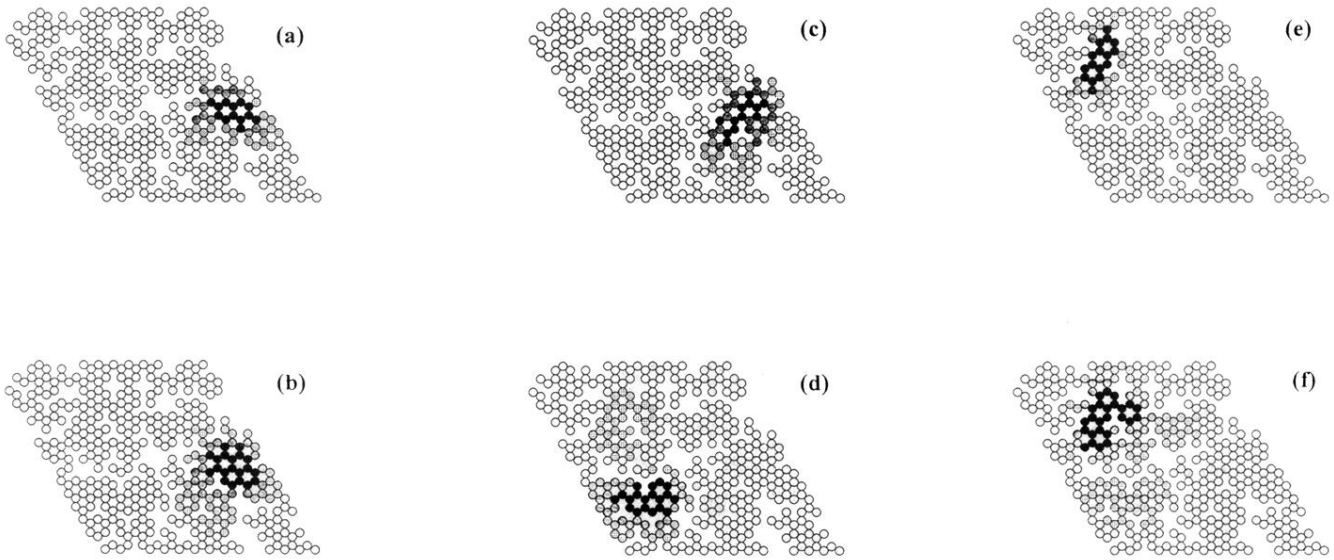

FIG. 3. Amplitudes of the several eigenstates of the porous-silicon cluster consisting of 350 Si atoms; (a) HOMO, (b) LUMO, (c) second HOMO, (d) second LUMO, (e) third HOMO, and (f) third LUMO. The amplitudes are larger at the atoms shaded more darkly. The four classes of shading correspond to the regions of the amplitude from $\frac{1}{2}^{n+1}$ to $\frac{1}{2}^{n}$ of the maximum with $n=0$, 1, 2, and 3.

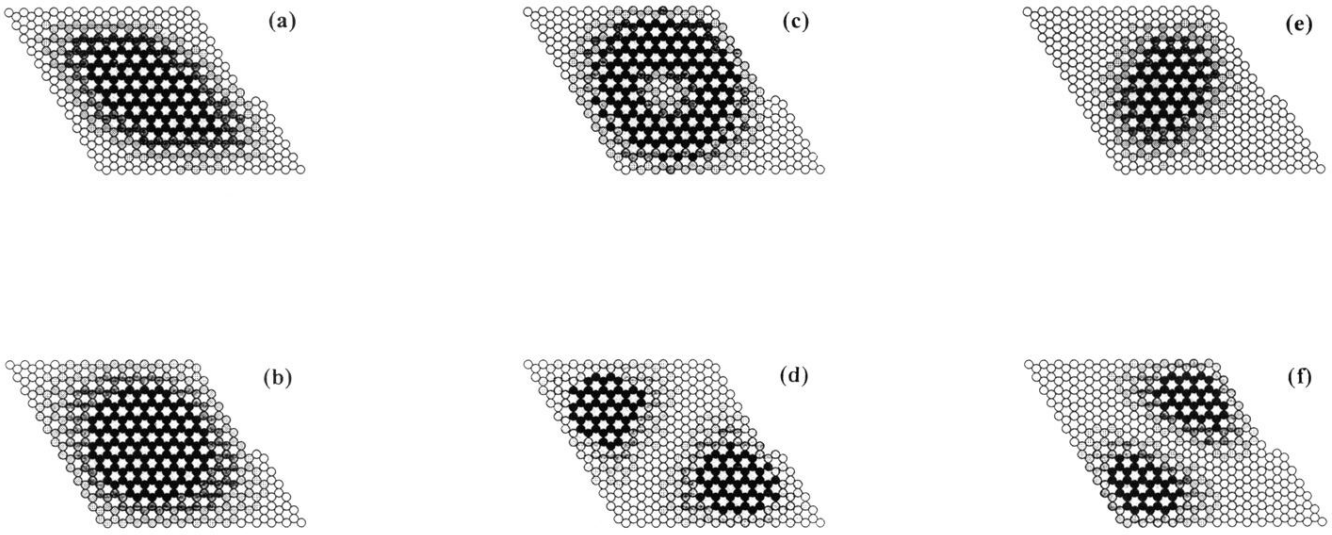

FIG. 4. The same as Fig. 3, except for the regular cluster consisting of 350 Si atoms.

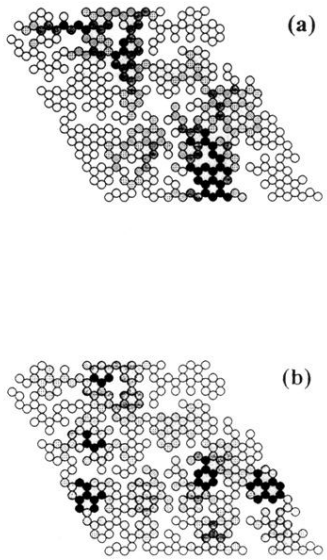

FIG. 7. The amplitudes of (a) the thirteenth HOMO and (b) the eighth LUMO for the porous-silicon cluster, which are indicated by the arrows in Fig. 5.